Scilight

Renewable Chemistry

https://www.sciltp.com/journals/rc

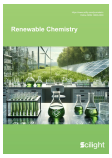

Article

One-Pot Technical Lignin Catalytic Depolymerization and Demethylation towards Valuable OH-Enriched Oligomers

Hugo Lilti, Lucile Olivier, Chantal Lorentz, Christophe Geantet and Dorothée Laurenti *

Institut de Recherches sur la Catalyse et l'Environnement de Lyon (IRCELYON), UMR 5256, CNRS-University Lyon 1, 2 Avenue Albert Einstein, 69626 Villeurbanne, France

* Correspondence: dorothee.laurenti@ircelyon.univ-lyon1.fr

How To Cite: Lilti, H.; Olivier, L.; Lorentz, C.; et al. One-Pot Technical Lignin Catalytic Depolymerization and Demethylation towards Valuable OH-Enriched Oligomers. *Renewable Chemistry* **2025**, *1*(1), 5.

Received: 5 August 2025
Revised: 16 September 2025
Accepted: 7 November 2025
Published: 14 November 2025

Abstract: The catalytic upgrading of technical lignin into valuable functional materials represents a key challenge for sustainable chemistry. This work presents a one-pot hydrogenolysis and demethylation process to transform Kraft lignin into hydroxyl (OH)-enriched oligomers suitable for bio-based polymer applications. Hydrogenolysis reactions were conducted using isobutanol as solvent and heterogeneous catalysts: $CoMo(O_x/S)/Al_2O_3$, $CoMo(O_x/S)/ZrO_2$, Mo_2C/C, and Pd/C. Products mixtures were separated into isobutanol soluble/insoluble and light/heavy fractions, and characterized by ^{31}P NMR, ^{13}C NMR, HSQC, and SEC. Among the selected candidates, alumina-supported CoMoS and $CoMoO_x$ were the most efficient. $CoMoS/Al_2O_3$ enhanced demethylation, producing catechol-type OH groups while $CoMoO_x/Al_2O_3$ favored depolymerization, generating more soluble oligomers but with lower demethylation. Light fractions were especially enriched in guaiacyl and catechol groups, while heavier ones retained more condensed C5 structures. These results confirm that demethylation and limited depolymerization (IUB ether bond cleavage) can be achieved, using a typical $CoMoS/Al_2O_3$ catalyst under hydrogenolysis conditions, primarily affecting smaller, soluble lignin-derivatives fragments. These fractions are promising intermediates for bio-based polyol for polymer synthesis, providing a sustainable route to valorize technical lignins using conventional hydrotreating catalysts.

Keywords: lignin; hydrogenolysis; catechol; catalysis; oligomers

1. Introduction

The need to find sustainable solutions to replace fossil resources is driving the development of new technologies for adding value to renewable resources, not only for fuels, but also for chemicals and materials. Lignin is an abundant natural component of biomass having an aromatic structure. However, the lignin co-produced in pulp industry or in cellulosic ethanol biorefinery is not valorized as such due to different reasons. The first one is the use of this lignin as a low-quality solid fuel to provide heat in the biorefinery. Nevertheless, much of the lignin co-produced can be valorized in other ways to improve sustainability of the processes and reduce overall carbon emissions [1]. Over the 100 million ton/year of lignin produced, it can be estimated that at least 10–20 wt% could be valorized as a by-product without hindering its utilization as a solid fuel in the industry [2]. The second issue is the versatility of the complex structure of those lignins. Contrarily to the lignins obtained from a lignin-first route, [3,4] where β-O-4 ether linkages are mostly preserved, as in native lignin, the technical lignin coming from cellulose extraction (e.g., pulp industry) shows increased C–C inter-units bonds (IUB) due to condensation reactions during the fragmentation process [5]. The depolymerization of such technical lignin into phenolic monomers or BTX compounds is therefore very complicated. Indeed, a way must be found to cut the C–C bonds in order to obtain the monomers, and so far, this problem has not been solved [6]. The use of lignin as a polyol in polymer synthesis was attempted and gave access

to new interesting bio-materials [7]. As well as bringing added value to lignin and reducing the polymer industry's dependence on fossil resource, the introduction of lignin into polyurethane foam, for instance, has resulted in improved mechanical properties, water, and UV resistance [5]. However, the direct use of technical lignin is never straightforward, mainly due to its versatility. Recent work has shown that functionalizing lignin OH groups can produce interesting new materials [8,9]. One solution for wider use would be to be able to provide lignin oligomers with a high OH concentration and narrower polydispersity. From previous studies, it was observed that lignin oligomers are often formed when the full depolymerization is attempted [10]. However, this research generally focuses on monomers, and the non-desired oligomeric fractions are generally neglected and poorly identified. This is understandable, given the difficulty of analyzing lignin oligomers fractions using conventional analytical tools. Most of the time, to get a clearer picture of oligomers structures, more powerful techniques like high resolution mass spectrometry like FTICR-MS or orbitrap are required [11–13]. In addition of mass spectrometry, methodologies using UV fluorescence were also attempted to determine oligomers ratio [14]. Centrifugal partition chromatography (CPC) proved to be an efficient technique for the separation and purification of monomers that could also be applied to oligomers [15]. The characterization of lignin monomers and small oligomers derivatives has recently been carried out using a powerful 2D LC x SFC method with tandem HRMS [16] which has enabled monomers, dimers, trimers and some tetramers to be cleverly separated and identified. A comparison of 2D LC x SFC analysis with GCXGC was also made showing clearly the complementarity of the two techniques [17]. One way to form oligomers with a technical lignin is to cleave all the residual ether inter-linkages bonds like β-O-4 and α-O-4. The ether bonds are easily cleaved compared to C–C bonds and lead to the formation of phenolics (Figure 1). Nevertheless, the low proportion of ether bonds between the units in technical lignins, can greatly limit depolymerization in this type of reaction. The demethylation of methoxy groups in lignin is also a C_{alkyl}-O bond cleavage in an aryl-alkyl ether function, which can be brought about by the same type of catalyst.

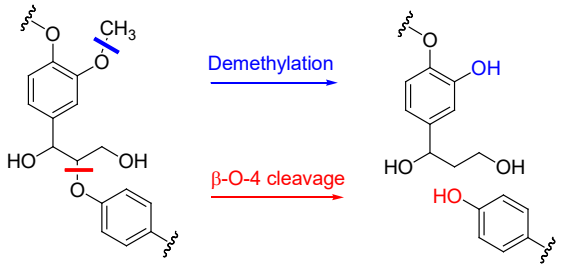

Figure 1. Demethylation and β-O-4 bond cleavage in lignin.

The only reported efficient lignin demethylation reaction was obtained by a homogeneous process using Iodocyclohexane [18]. There is obviously a way of improvement by developing a heterogeneous catalytic pathway that could realize both alkyl ether cleavage and demethylation to get lignin oligomers with a higher concentration of OH groups. Few heterogenous catalysis having performances towards partial depolymerization or demethylation of lignin were reported. The main ones were Ru/C [19], Ni/HZSM-5 [20] or Pd over different supports [21]. On model molecules, like guaiacol [22], anisole [23] or guaiacyl ethers [24], Lewis acidity has been found to improve demethylation but there are few examples on real lignin feeds [25].

In this work, we investigate the hydrogenolysis of a Kraft lignin with typical hydrotreating catalysts as a potential pathway to reach the OH-enriched oligomers target. We tested various catalysts for the depolymerization/demethylation of the lignin chosen according to our expertise on full depolymerization to monomers but also the literature on this topic. The demethylation extent was followed by quantifying remaining methoxy groups by ^{13}C NMR and catechol OH formed from guaiacyl units, that are the main phenolic units in the studied lignin, thanks to ^{31}P NMR after phosphitylation. To evaluate depolymerization, we characterized the oligomeric fractions by size-exclusion chromatography (SEC). Separating the products based on their affinity with the solvents used enabled us to determine the OH concentration in different light and heavier fractions. Since lignin contains a small amount of sulfur, and CoMo hydrogenolysis catalysts have proven to be effective, we compared $CoMoS/Al_2O_3$ catalyst with the oxide form, $CoMoO_x/Al_2O_3$ to evaluate whether the sulfide phase had a positive effect under these conditions.

2. Experimental Section

2.1. Materials

The lignin used in this work is a Kraft sample coming from Stora Enso.

$CoMoO_x/Al_2O_3$ and $CoMoS/Al_2O_3$ catalysts were prepared starting from a benchmark catalyst (from Axens, shape as extrudate length 2–10 mm; diameter 1.2 mm) having 14 wt% of MoO_3 and 3 wt% of CoO, a BET surface area of 210 m^2/g and pore volume 0.5 cm^3/g. For the oxide form, the precursor $CoMoO_x/Al_2O_3$ was simply calcined (450 °C, 2 h under air flow 40 mL/min, 5 °C/min). The $CoMoS/Al_2O_3$ was obtained by sulfidation of this precursor for 3 h at 400 °C (15% H_2S/H_2, 40 mL/min, 5 °C/min) which ensures a good sulfidation [10]. After cooling down to room temperature, the catalyst was treated 8 h under a flow of 40 mL/min of N_2 and stored under argon.

$CoMoO_x$ and CoMoS catalysts supported on zirconia were prepared by incipient wetness impregnation of a solution containing 1.1 g of $(NH_4)_6Mo_7O_{24}.4H_2O$ and 0.737 g of $Co(NO_3)_2.6H_2O$ in 2.7 mL of water on 5.6 g a monoclinic zirconia (Saint-Gobain) following a reported method [26]. After maturation for 6 h, the paste was dried at 80 °C for 8 h, calcined and sulfided as described above to get $CoMoO_x/ZrO_2$ and $CoMoS/ZrO_2$ with 14.7 wt% MoO_3 and 2.76% CoO.

Mo_2C/C catalyst was prepared according a reported procedure [27]. The activated carbon (AC) support (Norit from Sigma Aldrich 900 m^2/g) was crushed and sieved between 80 to 120 µm and dried at 80 °C overnight. 2 g of AC was impregnated by a solution containing 0.909 g of $(NH_4)_6Mo_7O_{24}.4H_2O$ and 13 mL of water. After the maturation overnight, the mixture was dried at 80 °C for 12 h. The catalyst is then carburized under a flow of 40 mL/min of N_2 at 450 °C (5 °C/min, 2 h), then 850 °C (2 °C/min, 2 h). The obtained solid containing 20 wt% Mo as checked by XRF, (theoretical value is 19.8 wt%) is stored under argon. Presence of Mo_2C phase was checked by XRD (Figure S9).

Pd/C (10 wt%) is a benchmark catalyst provided by Roquette (BET Surface area 800 m^2/g, Pd: 9.8 wt%); before catalytic depolymerization, the catalyst was reduced under 40 mL/min of H_2 for 1 h at 400 °C with a heating rate of 1 °C/min.

2.2. Methods

Hydrogenolysis reaction. In a typical experiment, lignin (2.5 g) is fed into a 100 mL batch reactor with 40 mL isobutanol (IBol) and 10 wt.% catalyst (0.25 g). The reactor is sealed and flushed with nitrogen, followed by 3 successive pressurizations and evacuations to remove air. The reactor is heated to 280 °C (10 °C/min). Once the temperature has been reached, H_2 is introduced to reach a total pressure of 90 bar, and the timer is started. After 2 h reaction, the liquid fraction is recovered by filtration and the solid washed with THF to completely recover the oligomeric fraction. The two liquid fractions are combined and the solvents removed by rotary evaporation to weight the products (Figure S1). To separate roughly monomers and oligomers, the product fraction (100 mg) was solubilized in a small volume of acetone (0.5 mL). When n-heptane is then added (5 mL) to the mixture, the heavy fraction precipitates and is recovered after filtration. The heavy fraction is washed with heptane and dried. The light fraction is recovered after evaporation of the heptane and acetone solvents (Figure S1).

2.3. Characterization Techniques

^{31}P NMR analyses were done on a 400 MHz Bruker spectrometer. The quantification and discrimination of hydroxyl groups was realized after phosphitylation as described elsewhere [28]. Roughly, 20 mg of samples were dissolved in 300 µL of solution A (anhydrous pyridine: $CDCl_3$ at a ratio of 1.6:1 (*v*:*v*)), 200 µL of DMF, 100 µL of internal standard solution (20–30 mg/mL of cyclohexanol in solution A), 100 µL of relaxation reagent solution ($Cr(acac)_3$; 5 mg/mL in solution A) and 100 µL of 2-Chloro-4,4,5,5-tetramethyl-1,3, 2-dioxaphospholane (CTMDP). In addition of the classical regions for carboxylic, aliphatic, guaiacyl, syringyl and C_5 condensed OH, catechol OH were set between 139.2 and 138.3 ppm according to the signals observed for model molecules and the curves shape (Figure S2). ^{13}C NMR spectra were performed with a 1 Ghz Bruker apparatus for the initial lignin and on the 400 MHz for the depolymerized samples. The samples were prepared by accurately weighing around 100 mg of lignin sample and 10 mg of tetramethylthiourea (internal standard), with 5 mg $Cr(acac)_3$ and dissolved in DMSO-d_6. The sample is set at 50 °C for 2 h to allow fully dissolution. The HSQC spectra were obtained on a Bruker 400 Hz. For each sample, 80 mg of lignin is dissolved in 0.8 mL of DMSO-d_6 (the sample is heated at 45 °C for approximately two hours to allow full dissolution). The peak used for reference was the peak of DMSO which was set at (δC = 39.5 ppm, δH = 2.49 ppm). The phase of the two axes were adjusted in reference of the three highest peaks (which generally are the methoxy peak (δC = 55.3 ppm, δH = 3.70 ppm) the G_5 peak (δC =

115 ppm, δH = 6.6 ppm) and DMSO. The region assignments used for the quantification of the IUB are taken from previous articles [29,30].

The molecular mass distribution is determined thanks to size exclusion chromatography (SEC). Samples are prepared by dissolving 10 mg of lignin or derivatives in 1,5 mL of THF; the solution is then filtered through a 0,45 µm syringe filter to remove THF-insoluble part. The columns used are the Agilent PLGEL MIXED-D 5 µm × 2 and PLGEL 3 µm, and the flow is set to 1 mL/min and the detector is a Refraction Index Detector (RID). The retention time is converted to Polystyrene equivalent (PS eq.) thanks to calibration with polystyrene molecules of known molecular mass. The signal is then normalized so that the integration of the signal over the whole curve surface equals 1. The CHONS elemental analyses were performed on a Flash 2000 ThermoFisher apparatus; the carrier gas used is Helium and the detector used was a Thermal Conductivity Detector (TCD) and X-ray fluorescence (XRF) analysis was realized on a Panalytical Epsilon 4 instrument.

3. Results and Discussion

The Kraft Lignin *(*KL) used in this study has been characterized by TGA, NMR, SEC and elemental analyses. The main results are shown in Table 1. Classical CHONS elemental composition was found with 1.8 wt% of sulfur as expected for a Kraft sample. Ashes measured by TGA under air are around 1 wt% while the weight loss under N_2 is 27.3 wt% at 800 °C (Figures S3a,b). Carbon NMR shows high aromatic proportion C_{arom}/C_{aliph} = 4.6 and 1 C–O bond in each aromatic unit compared to 2 C–C bonds which indicates fairly strong condensation between the aromatic units (detailled quantification is given in Table S1). The total OH concentration measured by ^{31}P NMR in initial lignin is 6.37 mmol/g, including 3.96 mmol/g of aromatic OH, mostly condensed (1.7 mmol/g), guaiacyl/catechyl (2.1 mmol/g) and few hydroxyphenyl (0.17 mmol/g). The KL is slightly acid (pH = 3.95 when 2.5 g are dropped in 40 mL of water).

Table 1. Main characteristics of Lineo kraft lignin.

C wt%	**H wt%**	**O wt%**	**N wt%**	**S wt%**	**Ashes**
64.2	5.4	24.3	ND	1.8	4.4 * (1.0 $)
^{31}P NMR (mmol/g) OH					
Aliph. OH	Condensed. + S-units	Guaiacyl-units	Catechol-units	H-units	COOH	Total Arom. OH
2.11	1.7	1.69	0.41	0.17	0.43	3.96
^{13}C NMR (1 GHz)			2D HSQC (per 100 units)		
Aliph. C	Arom. C	OMe	α-β-O-4	α-β5	α-ββ
9.3	71.7	4.6	6.8	1.3	1.9

* Deduced from CHNS, $ obtained by ATG.

The SEC of the acetylated KL indicates a M_W of 3200 g/mol PS eq. with a polydispersity of 4 while initial lignin without acetylation showed much lower masses demonstrating that acetylation allows KL heavy masses to solubilize in THF (Figure S4). The semi-quantitative HSQC analysis shows that KL has typically mainly guaiacyl units, as expected for a softwood lignin, and still has a non-negligeable β-O-4 content and C–C bond IUB. These quantifications are in good agreement with what can be found in the literature [27].

In preliminary experiments (not reported here) done on a soda-type lignin, several catalytic systems were tested in hydrogenolysis conditions, but few of them had a significant impact in comparison with the reaction realized without catalyst. Among the systems having an effect, we found that typical hydrotreating catalysts based on a CoMo phase were among the most interesting. Traditional hydrogenolysis catalysts, like $CoMoS/Al_2O_3$ or $NiMoS/Al_2O_3$, were previously evaluated for the full depolymerization of lignin to monomers [10,31]. The utilized operating conditions ($P(H_2)$: 80 bar, 350 °C) allowed to obtain 17 wt% of monomers and around 35 wt% of oligomers with quite high deoxygenation level. In order to limit the deoxygenation and deep depolymerization (C–C bonds cleavage), while still being able to activate H_2, the temperature was set at 280 °C. In addition, to avoid as much as possible recondensation reactions, a strong supply of H_2 is essential. Besides H-donor tetralin/naphthalene solvent systems, that have been successfully used for full lignin depolymerization to monomers [10,30] but could complicate much the work-up and analysis, alcohols are generally used [32]. Here, we found that isobutanol (iBol) was the best compromise to perform depolymerization in the liquid phase without interacting with the products as proved by GCXGC analysis on the light fraction that does not show isobutanol incorporation in the products or a few [17].

Besides CoMo catalysts, we also tested Mo carbide and Pd/C catalysts that were found active for demethylation in previous works [33]. The mass yields of THF-soluble and insoluble fractions obtained for the

depolymerization reactions performed with the different catalysts are presented in Figure 2. The THF-soluble fractions yields are between 73 wt% to nearly 90 wt% for the reactions with and without catalyst. The losses are mainly due to the gases being formed and not recovered and the evaporation of light compounds while removing the THF and iBol solvents. Similar mass balances were found in the literature in close conditions [34,35]. In each case, the gas phase (analyzed by μGC) is mainly composed of CO_2. The insoluble yield was obtained by weighing the solids after reaction and subtracting the catalyst mass. The size-exclusion chromatograms of the THF-soluble fractions show the molecular masses distribution obtained for those experiments (Figure 3). For all depolymerization experiments, with or without catalyst, a shift toward lower masses was observed. However higher masses are still present, and the values obtained for Mw are higher than for initial lignin. The use of $CoMoS/Al_2O_3$ catalyst shows clearly a higher decrease of the heavier masses and a lower polydispersity.

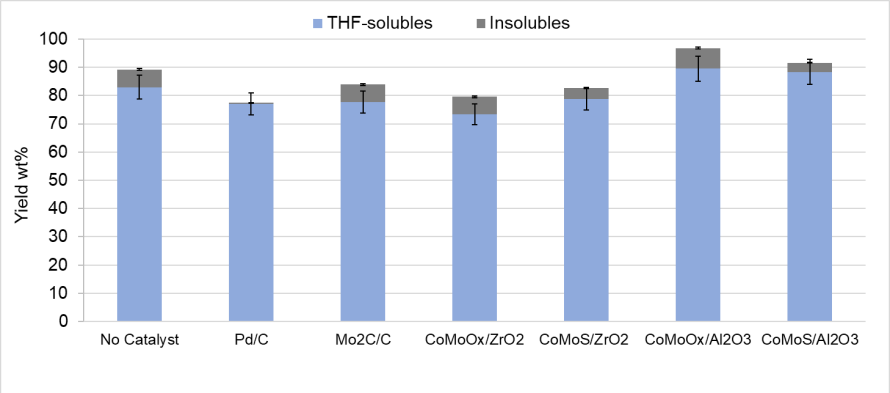

Figure 2. THF-soluble and THF-insoluble fractions yields recovered after reaction with or without catalyst.

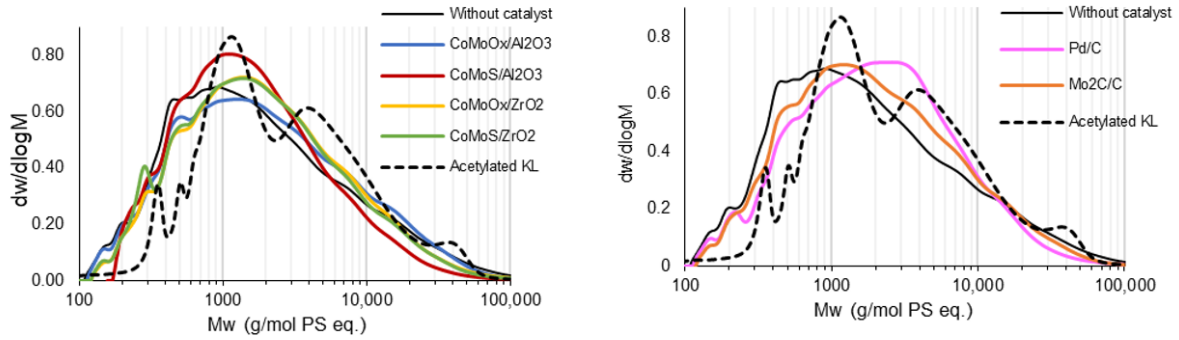

SEC	Mn (g/mol PS eq.)	Mw (g/mol PS eq.)	PDI
Without catalyst	856	5000	5.8
Pd/C	1033	4200	4.1
$CoMoO_x/Al_2O_3$	919	5014	5.5
$CoMoS/Al_2O_3$	932	3332	3.6
Mo_2C/C	994	4490	4.5
$CoMoO_x/ZrO_2$	999	4542	4.5
$CoMoS/ZrO_2$	960	4307	4.5
Acetylated KL	788	3240	4.1

Figure 3. Size-exclusion chromatograms of the various THF-soluble fractions and acetylated KL with the corresponding average molecular masses (Mw) in g/mol PS eq. and polydispersity indexes (PDI).

The ^{31}P NMR analysis applied for the hydroxyl-groups quantification of the THF-soluble fractions indicates an increase of total aromatic OH groups in nearly all the products (Figure 4) except for the non-catalyzed and Pd/C-catalyzed experiments. As the products were in contact with iBol solvent, the aliphatic OH groups are not reported to avoid any confusing result even if the solvent was removed. The greater increase in total aromatic and catechol OH groups was measured for the fractions obtained with the alumina-supported CoMoS and $CoMoO_x$

catalysts. CoMoS catalyst on zirconia support, that was very efficient in promoting the direct demethoxylation of guaiacol to phenol, in HDO of model molecule [26] shows only a slight increase of the hydroxyls concentration. The interest for oxophilic zirconia support for those $CoMoO_x$(S) phase appears to be limited here compared to alumina. Carbon-supported Mo carbide catalyst did not show any improvement for depolymerization or demethylation steps, unlike to what was previously reported in literature with similar catalysts [36]. Carboxylic OH decreased after depolymerization whatever the experiment, confirming that decarboxylation reaction occurred at quite low temperature (from 200 °C), with or without catalyst, in coherence with the CO_2 found as the main component of the gas phase. For comparison purpose, we realized the homogeneous demethylation reaction with Iodocyclohexane on KL according to the reported method [18]. This homogeneous demethylation step resulted on total aromatic OH groups quantification of 5.3 mmol/g, with a strong increase of catechol OH, which is obviously higher than the values obtained here by catalytic hydrogenolysis reaction (Figure S5).

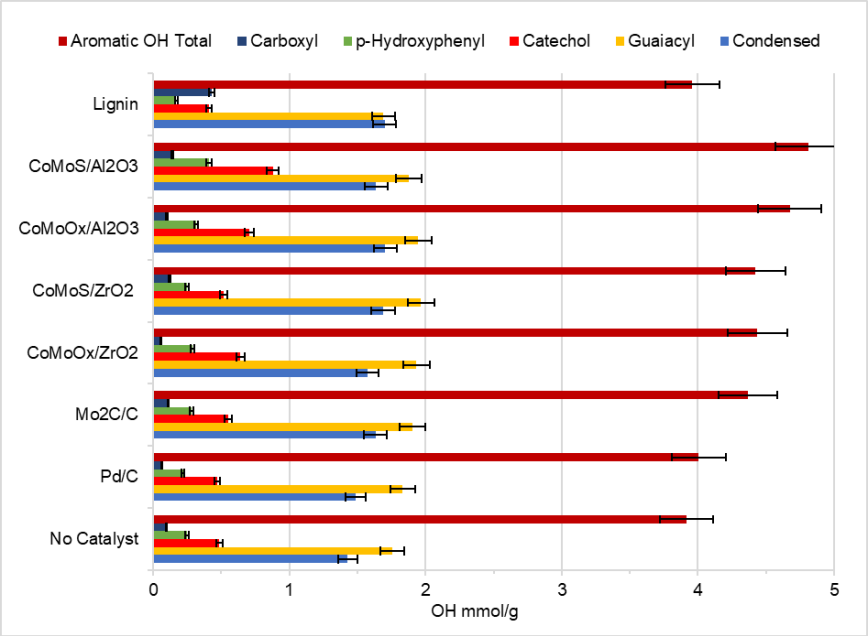

Figure 4. Hydroxyl groups quantification by ^{31}P NMR for the THF-soluble fractions and KL.

The decrease of ether IUB and methoxy groups in the depolymerized THF-fractions was observed by HSQC and ^{13}C NMR analyses respectively (Table S2). Alumina-supported CoMoS catalyst shows the higher decrease of those ether functions, while zirconia-supported one indicates an increase compared to initial lignin. However, for all catalytic experiments, the decrease in methoxy groups, characteristic of guaiacyl units, is correlated with the increase in catechols (Figure S6). However, the variation of the concentration of each is not in the same range. Evaluating methoxy groups reduction as a marker of demethylation is an important step, but quantification of methoxy groups by ^{13}C or HSQC in such a complex structure is only semi-quantitative, and comparison with lignin may be inappropriate as we only analyzed the THF-soluble fraction after reaction. Furthermore, demethylation can take place on G (guaiacyl) units whereas depolymerization by ether IUB cleavage does not occur (see Figure 1 blue OH), and, therefore lead to produce phenolic OH groups instead of catechol as seen for $CoMoS/Al_2O_3$ (Table S2). Finally, methoxy groups can also be removed by demethoxylation, although this deoxygenation reaction generally requires higher temperature [37].

Since the impact of catalysts was still unclear, we investigated whether the catalyst is ineffective or if only small molecules can interact with it, as opposed to larger ones, potentially due to solubility or diffusion limitations, as shown in other studies [38,39]. To achieve this, for the most interesting catalysts, i.e., $CoMoO_x/Al_2O_3$ and $CoMoS/Al_2O_3$, we first isolated only the soluble fraction in iBol after the reaction without addition of THF-extracts. Although the solubility at the reaction temperature differ from that at room temperature, it is reasonable to assume that all molecules soluble at room temperature remain soluble at 280 °C. Consequently, the iBol-soluble phase is composed exclusively of molecules that are soluble at higher temperatures and can interact with the catalyst during the reaction. For alumina-supported CoMoS and $CoMoO_x$ catalysts, this fractionation showed respectively that 32.6 wt% and 60.6 wt % of the starting lignin are soluble in iBol solvent (Table 2). Thus, much less oligomeric compounds appeared to be formed or solubilized with sulfided CoMo catalyst compared to the CoMo oxide. However, the solubility is not only linked with molecular size but might also depend on the type of

chemical function, in particular, if OH groups concentration is increased, the solubility of monomers and oligomers could also be limited.

Table 2. Mass balance obtained with iBol direct separation and catechol and total aromatic OH in iBol-Sol fraction.

	iBol-Soluble wt%	iBol-Insoluble wt%	Catechol OH (mmol/g) in iBol-Soluble	Arom OH (mmol/g) in iBol-Soluble
$CoMoO_x/Al_2O_3$	60.6	38.8	0.79	5.35
$CoMoS/Al_2O_3$	32.6	64.8	1.03	5.35

The catechyl and guaiacyl OH groups increased in the iBol fraction obtained with both catalysts compared to the whole soluble fraction in THF while condensed OH (β-5, 5-5, 4-O-5) concentration decreased (Figure 5). Both catalysts lead to the same total aromatic OH amount, that represent an increase of 35% compared to KL, however, with higher guaiacyl concentration with CoMo oxide while the CoMo sulfide catalyst led to higher catechyl concentration.

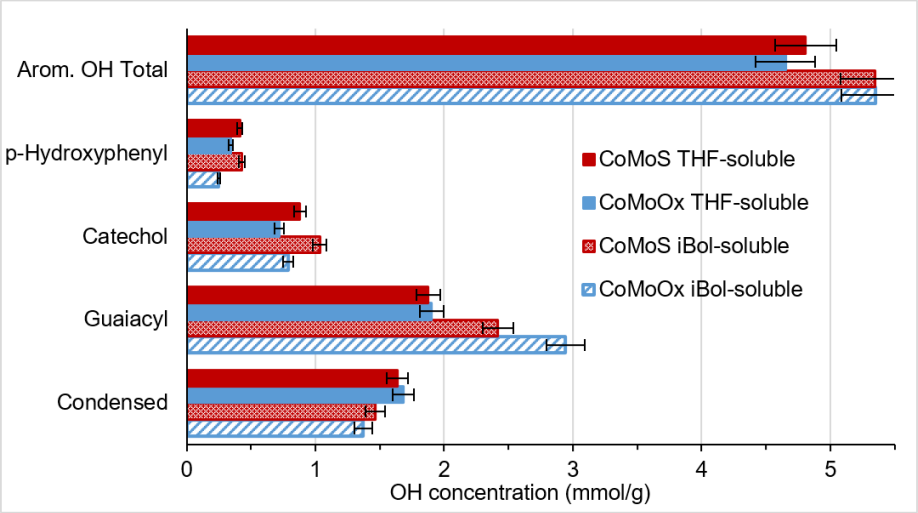

Figure 5. Comparison of OH quantification in iBol-soluble and THF-soluble fractions for $CoMoS/Al_2O_3$ and $CoMoO_x/Al_2O_3$ catalysts.

Those results suggest a higher depolymerization with $CoMoO_x$ in accordance with the higher iBol soluble yield, but a lower demethylation extent compared to CoMoS catalyst. The SEC analysis of the iBol fractions shows a clear decrease of the polydispersity and masses for the iBol fractions compared to the whole THF-soluble fractions for both catalysts (Figure 6). The fraction obtained with CoMoS catalyst appears a bit narrower compared to the one with $CoMoO_x$. Finally, for this iBol fraction, the impact of the catalysts is more clearly observed with a decreased Mw and PDI and increased OH concentration, indicating that iBol fraction solubilizes the lighter oligomers that were more easily converted than longer oligomers. This also means that the iBol solvent can solubilize small oligomers having OH groups like catechol moiety. With CoMoS catalyst, for instance, iBol fraction has 1.03 mmol/g of catechol units while according to the mass balance (32 wt%), it should contain only 0.28 mmol/g of catechol, if it was separated without size effect. Apart from the solvent impact, the main conclusion from these separation experiments is that $CoMoS/Al_2O_3$ is more selective for demethylation as catechol groups were measured in higher amount.

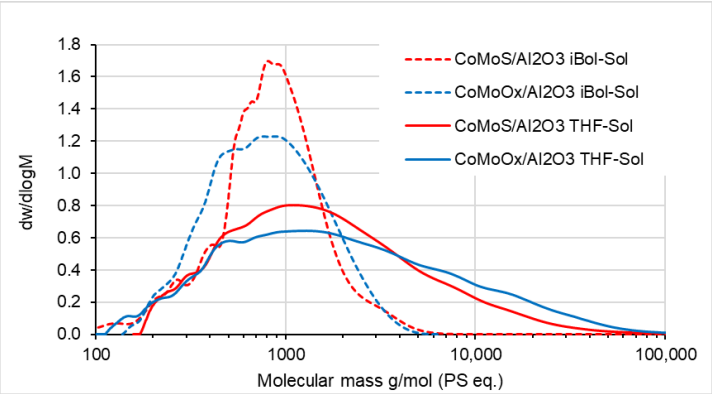

Figure 6. SEC curves of iBol fractions compared to the whole THF-soluble fractions and average molar masses (PS eq) and polydispersity (PDI).

In order to go further, the whole THF-soluble products were fractionated into light and heavy fractions by acetone/heptane precipitation according to the described protocol (Figure S1). For both catalysts, the light fraction represents around 25 wt% of the whole soluble fraction (Table 3). A similar light fraction, that was obtained by the same procedure and catalyst, but starting with a soda lignin, was previously analyzed thanks to comprehensive LCxSFC technique, and showed the presence of monomers, dimers, trimers and few tetramers [16]. In this previous work, we observed clearly the presence of many catechyl monomers and dimers. Those were also observed by GCXGC-TOF while comparing the two analytical techniques for the characterization of the same previous light sample [17]. The aromatic OH concentrations for light and heavy fractions are given in Figure 7. Higher guaiacyl and catechyl OH concentration is found in the lighter fraction for both catalysts, even more pronounced for catechol OH with the CoMoS catalyst, and a decrease of OH groups on condensed units contrarily to heavy fractions. Hydroxy-phenolic groups are in similar concentration for light and heavy fractions. If we sum the catechol OH in heavy and light fractions in proportion of the mass balance of those fractions, the extrapolated catechol OH value is slightly lower but in the same range than the concentration in the THF-soluble fraction which shows that the distribution after the separation is coherent (Table 3). Thus, this is again confirming the higher ability of the CoMoS catalyst for the demethylation step. The similar concentration of p-hydroxyphenyl OH groups in both heavy and light fractions contrarily to guaiacyl indicate that phenolic OH groups were simultaneously increased in small and large oligomers, probably by depolymerization i.e ether inter-units cleavage, while guaiacyl formation (ether inter-unit cleavage in G units) is occuring mostly in small oligomers.

Table 3. Mass balance obtained by fractionating the whole THF-soluble fraction into a light and heavy fraction with quantified catechol OH in those fractions by extrapolation and measurement.

Catalysts	Heavy Fract. wt% [Cat. OH mmol/g]	Light Fract. wt% [Cat. OH mmol/g]	Cat. OH [a] (mmol/g)	Cat. OH in THF-Soluble [b] (mmol/g)
$CoMoS/Al_2O_3$	73.3 [0.56]	26.7 [1.32]	0.76	0.88
$CoMoO_x/Al_2O_3$	76.2 [0.61]	23.8 [0.92]	0.68	0.71

[a] Calculated by summing quantities in heavy and light fractions; [b] measured in THF-soluble fraction.

An overview of all the OH quantification in the various fractions obtained with $CoMoO_x$ and CoMoS catalysts is presented in Figure S7. That shows clearly that heavy fractions contain more condensed C5 OH while guaiacyl and catechol OH groups are in greater amount in light fractions. The SEC curves realized on light and heavy fractions (Figure 8) confirmed the good separation of the molecules according to their masses for CoMoS catalyst. The same is observed for oxide system (Figure S8). The light and iBol-soluble fractions obtained with both catalysts are similar in terms of masses and polydispersity. The light fractions present much lower masses compared to the iBol fractions. The molecular masses in light fractions were divided by a factor of 2 while the polydispersity indexes are similar (Table 4).

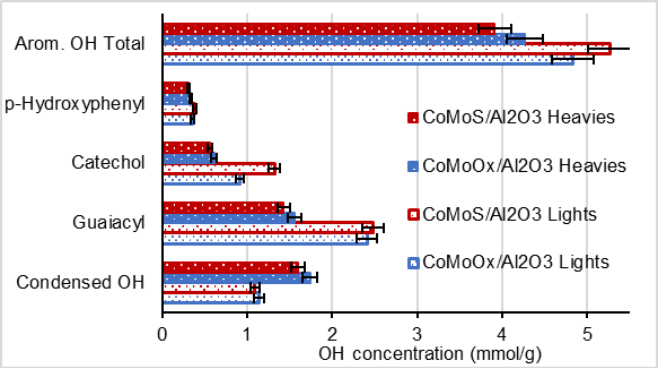

Figure 7. Aromatic hydroxyl concentration in the light and heavy fractions with alumina-supported $CoMoO_x$ and CoMoS.

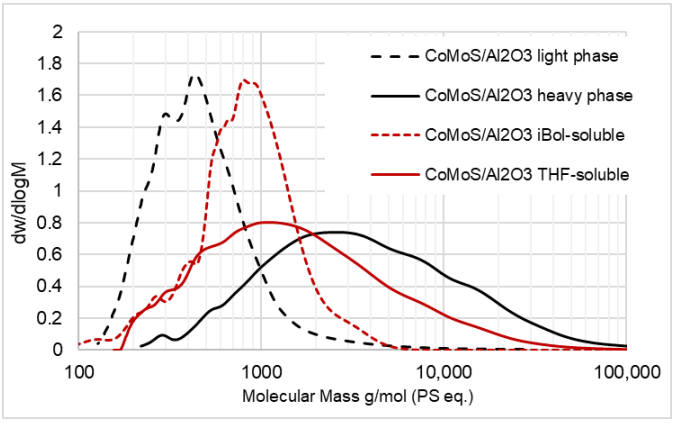

Figure 8. SEC curves of light, heavy fractions compared with THF- and iBol-soluble fractions for $CoMoS/Al_2O_3$ catalyst.

Table 4. Average mass (Mw) and Polydispersity (PDI) for IBol and light fractions obtained with $CoMoO_x/Al_2O_3$ and $CoMoS/Al_2O_3$.

Fraction	Mw g/mol	PDI
$CoMoO_x/Al_2O_3$ iBol	980	1.55
$CoMoS/Al_2O_3$ iBol	924	1.34
$CoMoO_x/Al_2O_3$ Light	568	1.41
$CoMoS/Al_2O_3$ Light	619	1.57

Finally, the light fractions are mainly composed of monomers and dimers, and, the total aromatic OH concentration in light fractions is slightly lower than the one measured in iBol fractions. This is underlining the interest for the iBol fraction which is the easier to recover just after the reaction and without additional solvent and presents a greater aromatic OH concentration. This also clearly shows that the heavier oligomers contained in THF-soluble fraction did not react well with heterogeneous catalysts in hydrogenolysis operating conditions. The Kraft lignin used here has a condensed structure, and the presence of large, tangled macromolecules limits contact with catalytic sites.

Surprisingly, the extruded catalysts were completely destroyed after the reaction, while the same type of extrudates were used in more severe operating conditions without any damage in tetralin. This is probably due to the use of iBol solvent. So it was not possible to analyze the used catalysts separately. The entire solids obtained after reaction, including the catalysts, were thus analyzed by CHNS elemental analyses (Table S3) and showed similar amounts of residual carbon (21–25 wt%). Interestingly, S was not detected on the remaining solid with $CoMoO_x$ catalyst indicating that the S initially measured in KL is not transfered onto the catalyst during the reaction under these operating conditions.

4. Conclusions

The study presented here aimed to investigate the catalytic hydrogenolysis reaction for the conversion of kraft lignin into oligomers enriched with aromatic hydroxyl groups. Among the catalysts tested, the typical hydrotretaing catalyst, i.e., CoMo-based systems, exhibited the most promising results in terms of depolymerization and demethylation efficiency. The $CoMoS/Al_2O_3$ catalyst, in particular, favored the formation of catechol-type hydroxyl groups, indicating selective demethylation of guaiacyl units, while $CoMoO_x/Al_2O_3$ showed a stronger depolymerization effect leading to higher solubility and lower molecular weights. Fractionation and spectroscopic analyses confirmed that light oligomeric fractions were enriched in aromatic hydroxyl groups, especially catechols and guaiacyl units, while condensed structures dominated in heavier fractions. The results demonstrate that it is possible to partially depolymerize technical kraft lignin while increasing its hydroxyl functions through a heterogeneous catalytic process under hydrogenolysis conditions. These findings highlight the potential of CoMoS catalysts for the selective transformation of technical lignin into functional OH-enriched fractions with enhanced reactivity. Howeve, these are more monomers and dimers than longer oligomers. The isobutanol-soluble fraction, that is the easier one to recover after reaction and contains the greater aromatic OH concentration, constitutes an interesting oligomeric fraction for a subsequent OH group functionalization step towards functionalization and subsequent polymerization. Future work should focus on catalyst stability, solvent effects, and the optimization of reaction parameters to improve yield and selectivity toward well-defined oligomeric bio-based building blocks.

Supplementary Materials

The additional data and information can be downloaded at: https://media.sciltp.com/articles/others/25111415 47382095/RC-2508000202-Supplementary-materials-FINAL.pdf. Figure S1: Products-recovery protocol for hydrogenolysis reactions. Figure S2: ^{31}P NMR Spectra: in red, iBol fraction after depolymerization with $CoMoS/Al_2O_3$; in blue, iBol fraction with $CoMoO_x/Al_2O_3$; the green and blue rectangles are the zones defined for guaiacol and catechol functions respectively—Catechol molecule is having one peak at 139 ppm. Figure S3a: Thermogravimetric analysis under air. Figure S3b: Thermogravimetric analysis under N_2. Figure S4: Size-Exclusion Chromatography analysis of KL and acetylated KL. Figure S5: ^{31}P NMR OH groups quantification after demethylation with homogeneous method. Figure S6: Correlation between methoxy (^{13}C NMR) and catechol OH (^{31}P NMR) groups for the various fractions. Figure S7: Quantification of aromatic hydroxyl groups in the THF-, iBol, Light and heavy fractions for alumina-supported CoMoOx and CoMoS catalysts. Table S1: Quantification of carbon functional groups thanks to ^{13}C NMR (done with the 1GHz spectrometer) Table S2: NMR analyses result for β-O-4 units, methoxy, catechol OH and phenol OH groups of THF-soluble fractions obtained with and without catalyst and compared to initial KL. Table S3: Elemental analysis of solids obtained with $CoMoOx/Al_2O_3$ and $CoMoS/Al_2O_3$ catalysts, including the catalysts that could not be removed.

Author Contributions

H.L.: methodology, data curation, writing—original draft preparation; visualization, investigation; writing—reviewing and editing; L.O.: methodology; data curation; investigation; C.L.: methodology; data curation; validation; C.G.: investigation; supervision; D.L.: conceptualization, methodology, writing—original draft preparation; visualization; investigation; supervision; writing—reviewing and editing. All authors have read and agreed to the published version of the manuscript.

Funding

Funding source is already indicated in Aknowledgment section ANR BIOPOLIOL project (ANR-21-CE43-0026).

Institutional Review Board Statement

Not applicable.

Informed Consent Statement

Not applicable.

Data Availability Statement

We advocate for the sharing of research data by all authors contributing to publications in Scilight journals. In this section, authors may be asked to provide the raw data of their study together with the manuscript for editorial review and should be prepared to make the data publicly available if practicable. In any event, authors should ensure accessibility of such data to other competent professionals for at least 10 years after publication (preferably via an institutional or subject-based data repository or other data center), provided that the confidentiality of the participants can be protected and legal rights concerning proprietary data do not preclude their release. In instances where novel data were not generated or data remains inaccessible due to privacy or ethical considerations, a clear statement outlining these circumstances is mandatory.

Acknowledgments

The authors warmly thank the ANR for funding the BIOPOLIOL project (ANR-21-CE43-0026) and the four other project partners (ISA, ICPEES, ABI and SOPREMA) for the fruitful discussions at project meetings.

Conflicts of Interest

No conflict of interest.

Use of AI and AI-Assisted Technologies

Use of AI only for improving some text with Deepl free software.

References

1. Sethupathy, S.; Morales, G.M.; Gao, L.; et al. Lignin valorization: Status, challenges and opportunities. *Biores. Tech.* **2022**, *347*, 126696. https://doi.org/10.1016/j.biortech.2022.126696.
2. Bajwa, D.S.; Pourhashem, G.; Ullah, A.H.; et al. A concise review of current lignin production, applications, products and their environmental impact. *J. Ind. Crops* **2019**, *139*, 111526. https://doi.org/10.016/j.indcrop.2019.111526.
3. Zijlstra, D.S.; Analbers, C.A.; de Korte, J.; et al. Efficient Mild Organosolv Lignin Extraction in a Flow-Through Setup Yielding Lignin with High β-O-4 Content. *Polymers* **2019**, *11*, 1913. https://doi.org/10.3390/polym11121913.
4. Renders, T.; Van den Bossche, G.; Vangeel, T.; et al. Reductive catalytic fractionation: State of the art of the lignin-first biorefinery. *Curr. Op. Biotech.* **2019**, *56*, 193–201. https://doi.org/10.1016/j.copbio.2018.12.005.
5. Khorshidi, F.H.; Najafi, S.K.; Najafi, F.; et al. The extraction of polyol for the synthesis of lignin-based polyurethane coatings—A review. *Wood Mater. Sci. Eng.* **2024**, *19*, 794–802. https://doi.org/10.1080/17480272.2024.2335502.
6. Luo, Z.; Liu, C.; Radu, A.; et al. Carbon–carbon bond cleavage for a lignin refinery. *Nat. Chem. Eng*. **2024**, *1*, 61–72. https://doi.org/10.1038/s44286-023-00006-0.
7. Laurichesse, S.; Avérous, L. Chemical modification of lignins: Towards biobased polymers. *Progr. Polym. Sc.* **2014**, *39*, 1266–1290. https://doi.org/10.1016/j.progpolymsci.2013.11.004.
8. Wybo, N.; Duval, A.; Avérous, L. Benign and selective amination of lignins towards aromatic biobased building blocks with primary amines. *Angew. Chem. Int. Ed.* **2024**, *63*, e202403806. https://doi.org/10.1002/anie.202403806.
9. Wybo, N.; Cherasse, E.; Duval, A.; et al. Unlocking sustainable, aromatic, and versatile materials through transurethanization: Development of non-isocyanate polyurethanes from lignins. *Mater. Chem. A* **2025**, *13*, 11557–11572. https://doi.org/10.1039/d4ta08582e.
10. Pu, J.; Nguyen, T.-S.; Leclerc, E.; et al. Lignin catalytic hydroconversion in a semi-continuous reactor: An experimental study. *Appl. Catal. B Env.* **2019**, *256*, 117769. https://doi.org/10.1016/j.apcatb.2019.117769.
11. Kosyakov, D.S.; Pikovskoi, I.I.; Ul'yanovskii, N.V. Dopant-assisted atmospheric pressure photoionization Orbitrap mass spectrometry–An approach to molecular characterization of lignin oligomers. *Anal. Chim. Acta* **2021**, *1179*, 338836. https://doi.org/10.1016/j.aca.2021.338836.
12. Letourneau, D.R.; Volmer, D.A. Mass spectrometry-based methods for the advanced characterization and structural analysis of lignin: A review. *Mass Spec. Rev*. **2023**, *42*, 144–188. https://doi.org/10.1002/mas.21716.
13. Sander, K.; Dütsch, L.; Bremer, M.; et al. Characterization of soluble and insoluble lignin oligomers by means of ultrahigh resolving mass spectrometry. *Energy Fuels* **2023**, *37*, 439−449. https://doi.org/10.1021/acs.energyfuels.2c03538.
14. Bartolomei, E.; Le Brech, Y.; Dufour, A.; et al. Lignin depolymerization: A comparison of methods to analyze monomers and oligomers. *ChemSusChem* **2020**, *13*, 4633. https://doi.org/10.1002/cssc.202001126.
15. Alherech, M.; Omolabake, S.; Holland, C.M.; et al. From lignin to valuable aromatic chemicals: Lignin depolymerization and monomer separation via centrifugal partition chromatography. *ACS Cent. Sci.* **2021**, *7*, 1831–1837. https://doi.org/10.1021/acscentsci.1c00729.

16. Tammekivi, E.; Batteau, M.; Laurenti, D.; et al. A powerful two-dimensional chromatography method for the non-target analysis of depolymerised lignin. *Anal. Chim. Acta* **2024**, *1288*, 342157. https://doi.org/10.1016/j.aca.2023.342157.
17. Tammekivi, E.; Lilti, H.; Batteau, M.; et al. Complementarity of two-dimensional gas chromatography and two-dimensional liquid chromatography for the analysis of depolymerised lignin. *J. Chrom. A* **2024**, *1736*, 465401. https://doi.org/10.1016/j.chroma.2024.465401.
18. Ferhan, M.; Yan, N.; Sain, M. A new method for demethylation of lignin from woody biomass using biophysical methods. *J. Chem. Eng. Process. Techn.* **2013**, *4*, 160. https://doi.org/10.4172/2157-7048.1000160.
19. Kozmelj, T.R.; Bartolomei, E.; Dufour, A.; et al. Oligomeric fragments distribution, structure and functionalities upon ruthenium-catalyzed technical lignin depolymerization. *Biomass Bioenergy* **2024**, *181*, 107056. https://doi.org/10.1016/j.biombioe.2024.107056.
20. Liu, X.; Jiang, Z.; Feng, S.; et al. Catalytic depolymerization of organosolv lignin to phenolic monomers and low molecular weight oligomers. *Fuel* **2019**, *244*, 247–257. https://doi.org/10.1016/j.fuel.2019.01.117.
21. Karnitski, A.; Choi, J.-W.; Suh, D.J.; et al. Roles of metal and acid sites in the reductive depolymerization of concentrated lignin over supported Pd catalysts. *Catal. Today* **2023**, *113844*, 411–412. https://doi.org/10.1016/j.cattod.2022.07.012.
22. Wu, X.; Liao, Y.; Bomon, J.; et al. Lignin-first monomers to catechol: Rational cleavage of C−O and C−C bonds over zeolites. *ChemSusChem* **2022**, *15*, e202102248. https://doi.org/10.1002/cssc.202102248.
23. Ji, N.; Wang, Z.; Diao, X.; et al. Highly selective demethylation of anisole to phenol over H 4 Nb 2 O 7 modified MoS 2 catalyst. *Catal. Sci. Technol.* **2021**, *11*, 800–809. https://doi.org/10.1039/D0CY01972K.
24. Jiang, L.; Guo, H.; Li, C.; et al. Selective cleavage of lignin and lignin model compounds without external hydrogen, catalyzed by heterogeneous nickel catalysts. *Chem. Sci.* **2019**, *10*, 4458–4468. https://doi.org/10.1039/C9SC00691E.
25. Podschun, J.; Saake, B.; Lehnen, R. Catalytic demethylation of organosolv lignin in aqueous medium using indium triflate under microwave irradiation. *React. Funct. Polym.* **2017**, *119*, 82–86. https://doi.org/10.1016/j.reactfunctpolym.2017.08.007.
26. Bui, V.N.; Laurenti, D.; Delichère, P.; et al. Hydrodeoxygenation of guaiacol. Part II: Support effect for CoMoS catalysts on HDO activity and selectivity. *Appl. Cat. B Env.* **2011**, *101*, 246–255. https://doi.org/10.1016/j.apcatb.2010.10.031.
27. Meng, S.; Xue, X.; Wenig, Y.; et al. Synthesis and characterization of molybdenum carbide catalysts on different carbon supports. *Cata. Today* **2022**, *402*, 266–275. https://doi.org/10..1016/j.cattod.2022.04.020.
28. Meng, X.; Crestini, C.; Ben, H.; et al. Determination of hydroxyl groups in biorefinery resources via quantitative 31P NMR spectroscopy. *Nat. Protoc.* **2019**, *14*, 2627–2647. https://doi.org/10.1038/s41596-019-0191-1.
29. Smit, A.T.; Dezaire, T.; Riddell, L.A.; et al. Reductive partial depolymerization of acetone organosolv lignin to tailor lignin molar mass, dispersity, and reactivity for polymer applications. *ACS Sustain. Chem. Eng.* **2023**, *11*, 6070–6080. https://doi.org/10.1021/acssuschemeng.3c00617.
30. Van Aelst, K.; Van Sinay, E.; Vangeel, T.; et al. Reductive catalytic fractionation of pine wood: Elucidating and quantifying the molecular structures in the lignin oil. *Chem. Sci.* **2020**, *11*, 11498–11508. https://doi.org/10.1039/D0SC04182C.
31. Joffres, B.; Lorentz, C.; Vidalie, M.; et al. Catalytic hydroconversion of a wheat straw soda lignin: Characterization of the products and the lignin residue. *Appl. Cat. B Env.* **2014**, *145*, 167–176. https://doi.org/10.1016/j.apcatb.2013.01.039.
32. Oregui-Bengoechea, M.; Gandarias, I.; Arias, P.L.; et al. Unraveling the role of formic acid and the type of solvent in the catalytic conversion of lignin: A holistic approach. *ChemSusChem* **2017**, *10*, 754–766. https://doi.org/10.1002/cssc.201601410.
33. Wu, X.; Smet, E.; Brandi, F.; et al. Advancements and perspectives toward lignin valorization via O-demethylation. *Angew. Chem. Int. Ed.* **2023**, *136*, e202317257. https://doi.org/10.1002/anie.202317257.
34. Chen, P.; Zhang, Q.; Shu, R.; et al. Catalytic depolymerization of the hydrolyzed lignin over mesoporous catalysts. *Bior. Tech.* **2017**, *226*, 125–131. https://doi.org/10.1016/j.biortech.2016.12.030.
35. Kloekhorst, A.; Heeres, H.J. Catalytic hydrotreatment of alcell lignin using supported Ru, Pd, and Cu catalysts. *ACS Sust. Chem. Eng.* **2015**, *3*, 1905–1914. https://doi.org/10.1021/acssuschemeng.5b00041.
36. Yang, X.; Feng, M.; Choi, J.-S.; et al. Depolymerization of corn stover lignin with bulk molybdenum carbide catalysts. *Fuel* **2019**, *244*, 528–535. https://doi.org/10.1016/j.fuel.2019.02.023.
37. Bui, V.N.; Laurenti, D.; Afanasiev, P.; et al. Hydrodeoxygenation of guaiacol with CoMo catalysts. Part I: Promoting effect of cobalt on HDO selectivity and activity. *Appl. Cat. B Env.* **2011**, *101*, 239–245. https://doi.org/10.1016/j.apcatb.2010.10.025.
38. Mañas, A.H.; Vilcocq, L.; Fongarland, P.; et al. Lignin catalytic oxidation by CuO/TiO2: Role of catalyst in phenolics formation. *Waste Biom. Valor.* **2023**, *14*, 3789–3809. https://doi.org/10.1007/s12649-023-02082-y.
39. Huda, M.M.; Rai, N. Effect of solvent on the interaction of lignin with a zeolite nanosheet in the condensed phase. *J. Phys. Chem. B* **2023**, *127*, 6767–6777. https://doi.org/10.1021/acs.jpcb.3c02085.